FUZZY MODELING OF GUNSHOT BRUISES IN SOFT BODY ARMOR

Ian Lee
Department of Electrical Engineering
University of Southern California
Los Angeles, California 90089, USA
Email: ianlee@usc.edu

Bart Kosko
Department of Electrical Engineering
University of Southern California
Los Angeles, California 90089, USA
Email: kosko@sipi.usc.edu

W. French Anderson
Gene Therapy Laboratories
University of Southern California
Los Angeles, California 90089, USA

***Abstract*— Gunshots produce bruise patterns on persons who wear soft body armor when shot even when the armor stops the bullets. An adaptive fuzzy system modeled these bruise patterns by their depth and width given a projectile's mass and momentum. The fuzzy system used rules with sinc-shaped if-part fuzzy sets and was robust against random rule pruning: Median and mean test errors remained low even after removing up to one fifth of the rules. Gunshot data tuned the additive fuzzy function approximator. The fuzzy system's conditional variance $V[Y|X = x]$ described the second-order uncertainty of the function approximation. Handguns with different barrel lengths shot bullets over a fixed distance at armor-clad gelatin blocks that we made with Type 250A Ordnance Gelatin. The bullet-armor experiments found that a bullet's weight and momentum correlated with the depth of its impact on armor-clad gelatin ($R^2 = 0.953$ and p-value < 0.001 for the null hypothesis that the regression line had zero slope). Related experiments on plumber's putty found that highspeed baseball impacts compared well to bullet-armor impacts for large-caliber handguns. A baseball's impact depth in putty correlated with its momentum ($R^2 = 0.93$ and p-value < 0.001). Baseball impact depths were comparable to bullet-armor impact depths: Getting shot with a .22 caliber bullet when wearing soft body armor resembles getting hit in the chest with a 40-mph baseball. Getting shot with a .45 caliber bullet resembles getting hit with a 90-mph baseball.**

I. MODELING SOFT-BODY-ARMOR BRUISE IMPACT

How does it feel to get shot while wearing soft body armor? One police officer described it as a sting while another officer described it as a "hard blow" [1]. Fig. 1 shows the bruise beneath the armor after a .44 caliber bullet struck a police officer's upper left chest. The armor stopped the bullet but the impact still injured soft tissue.

We examined the bruising effect with a fuzzy function approximator and a baseball analogy. Bullet impact experiments produced the bullet-armor bruise data that generated a quantitative bruise profile and a baseball-impact comparison. The bruise profile gave the depth and width of the deformation that a handgun bullet made on gelatin-backed armor for gelatin blocks that we made with Type 250A Ordnance Gelatin (from Kind & Knox Gelatin).

Few researchers have studied the relationship between the bruising effect and the so-called *backface signature* or the deformation in the armor's backing material after a gunshot [2]. Our bruise profile modeled the bullet-armor impact with the depth and width of the bruise as a blunt object that could injure soft tissue. The baseball analogy helped estimate gunshot impacts on armor. We found that a fast baseball could hit as hard as a large caliber handgun bullet on armor.

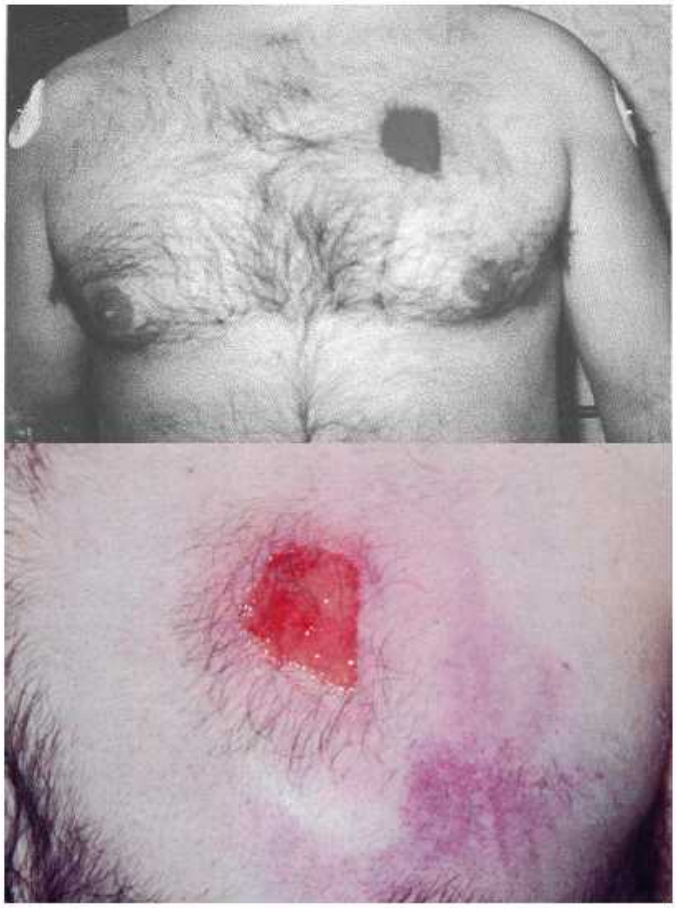

Fig. 1. **(a) Actual bruise from a police officer shot by a .44 caliber weapon in the line of duty while wearing soft body armor. (b) Close-up of the "backface signature" bruise in (a). Note that the bruise includes the discoloration around the wound. Photo reproduced with permission from the IACP/Du Pont Kevlar Survivors' Club.**

An adaptive fuzzy system learned to model the depth and width of bruise profiles from the bullet-armor impact experiments. The experiments found that a bullet made a larger impact if it had a larger caliber or a larger momentum (see Table 1). A larger and slower handgun bullet hit harder than a smaller and faster one in the experiments. Impact depth correlated better with momentum than with kinetic energy.

We picked the initial rules based on our ballistic judgment and experience. The experimental data tuned the rules of an adaptive standard-additive-model (SAM) fuzzy system [3]. The SAM system used two scalar subsystems to model the

Fig. 2. **One of the authors holds a 14-ply Kevlar soft body armor panel (from a Superfeatherlite vest from Second Chance) and some sample cartridges (.22, .38, .40, and .45 caliber). Different caliber bullets struck the sample armor but did not include a .44 caliber.**

depth and width of a bullet-armor impact in parallel given the bullet's weight and momentum. The fuzzy system was robust against random rule pruning. The median, mean, and maximal test errors resembled the initial system error for pruning that randomly removed up to 20% of the rules.

The next two sections review soft body armor and bullet-impact bruises.

II. SOFT BODY ARMOR

Soft body armor prevents most handgun bullets from penetrating a user's body [4]. Our armor experiments used a generic armor that combined many layers of fabric that wove together Kevlar fibers. Thinner armor is softer than thicker armor. Another type of armor material laminated together many layers of parallel fibers. Both types of armor deform under a bullet's impact and spread the impact's force over a wider area. Bullets penetrate by crushing [5]. So soft body armor arrests a handgun bullet by reducing its crushing force below a material-failure threshold [5].

Failure analysis does not consider the physiological effect as armor stops a bullet. Some researchers define armor failure as material failure such as broken fibers or breached fabric layers [6] – [10]. Others require complete bullet passages [11]. Such definitions do not address the interactions that flexible armor permit with the underlying material.

These interactions have two effects. The first is that a bullet-armor impact can injure soft tissue even though the bullets do not penetrate the armor (see Fig. 1). The second effect is that soft body armor's performance can differ for different "backing material" that supports the armor. We found that a hammer strike breached several layers of concrete-backed armor fabric but a handgun bullet bounced off gelatin-backed armor fabric.

The backface signature is the deformation in the backing material after a bullet strikes armor [5]. Studies of backface signatures [2] give little information about the impact as a bruising force if the backing material differs from soft tissue. One industry standard measures the backface signature on clay backing material [5]. The clay records the impact in a plastic or permanent deformation but its properties differ from soft tissue.

	MOMENTUM mv	WEIGHT m	KINETIC ENERGY $1/2\ mv^2$	SPEED v	WEIGHT & MOMENTUM $m\&v$
DEPTH	0.931	0.930	0.753	0.226 $p = 0.003$	0.953
WIDTH	0.952	0.877	0.836	0.140 $p = 0.025$	0.951

TABLE I. **Linear regression statistics (R^2) for the bullet impact experiments. Momentum correlated the most and kinetic energy correlated the least with an impact's depth and width. Speed correlated little with the impact's depth and width. A bullet's weight could represent its caliber because the experiments used one weight per caliber. All regression tests had p-value < 0.001 unless otherwise noted. The p-value measured the credibility of the null hypothesis $\mathbf{H}_0 : \beta_1 = 0$ that the regression line had zero slope β_1. A statistical test rejects the null hypothesis $\mathbf{H}_0$ at a significance level α if the p-value is less than that significance level. So the regression rejected the null hypothesis $\mathbf{H}_0$ for the customary significance levels $\alpha = 0.05$ and $\alpha = 0.01$ because p-value < 0.001.**

Gelatin tissue simulant is elastic and responds to a bullet's crushing force similar to how soft tissue responds in bullet penetration tests [12] – [14]. So testing gelatin-backed soft body armor can help study the armor's performance on a user's body. We performed the bullet-armor impact experiments on tissue simulant and defined a simple two-parameter bruise profile to describe the impact.

III. BRUISING AND THE BRUISE PROFILE

Bruising implies injury: It is escaped blood in the intercellular space after a blunt impact injures soft tissue [15]. The visible part of a bruise is the part of the escaped blood that is close to the skin surface. It need not indicate the severity of the injury. Scraping with a coin or a spoon can leave extensive but superficial bruises or welts that resemble bruises from abuse [16]. The visible bruise can change over time [17] at different rates based on sex, age, body fat [15], and medication [18]. So a bruise shows that a blunt impact occurred but need not show that internal injuries occurred [19], [20].

A bruise profile models the shape of the bullet-armor impact and can help guide the examination after an armor gunshot. The bruise profile can indicate the affected internal tissue beneath the visible armor bruise. We suggest that medical experts can infer the severity of internal injuries by applying the bruise profile based on a bullet's design, size, speed, and weight to the location of the bullet-armor impact.

IV. ADAPTIVE FUZZY SYSTEM

Bullet-impact experiments trained an adaptive fuzzy system to model the depth and width of the bullet-armor impact given a handgun bullet's weight and momentum. We picked the fuzzy system's initial depth rules in Table 2 based on the correlations in the experimental data (Table 1) and based on our ballistic judgment and experience. Similar rules described the width subsystem. A typical rule was "If a bullet's weight is very small (VS) and its momentum is small (SM) then the

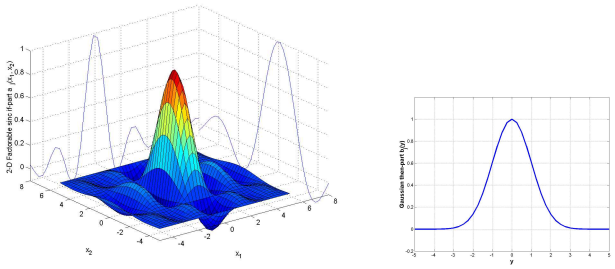

Fig. 3. **Sample if-part and then-part fuzzy sets. (a) Joint (product) sinc if-part set function for two-dimensional input case [21]. The joint set function has the factorable form $a_j(x) = a_j(x_1, x_2) = a_j^1(x_1) \times a_j^2(x_2)$. The shadows show the scalar sinc set functions $a_j^i : R \to R$ for $i = 1, 2$ that generate $a_j : R^2 \to R$. (b) Scalar Gaussian then-part set function.**

armor deformation depth is SM and the width is VS." The gunshot data tuned the rules in an adaptive standard-additive-model (SAM) function approximation.

We applied two scalar-valued additive fuzzy systems [3], [21] $F : R^2 \to R$ in parallel that used two-dimensional inputs to model the depth and width of a bullet-armor impact. These systems approximated some unknown function $f : R^2 \to R$ by covering the graph of f with m fuzzy rule patches and averaging patches that overlap. An if-then rule of the form "If X is A then Y is B" defined a fuzzy Cartesian patch $A \times B$ in the input-output space $X \times Y$. These nonlinear systems can uniformly approximate any continuous (or bounded measurable) function on a compact domain [3].

The SAM output computed a convex-weighted sum of the then-part centroids c_j for each vector input x

$$F(x) = \frac{\sum_{j=1}^{m} w_j a_j(x) V_j c_j}{\sum_{j=1}^{m} w_j a_j(x) V_j} = \sum_{j=1}^{m} p_j(x) c_j \tag{1}$$

for if-part joint set function $a_j : R^n \to [0, 1]$ that defined the if-part set $A_j \subset R^n$, rule weights $w_j \geq 0$, $p_j(x) \geq 0$, and $\sum_{j=1}^{m} p_j(x) = 1$ for each $x \in R^2$. The convex coefficient

$$p_j(x) = \frac{w_j a_j(x) V_j}{\sum_{i=1}^{m} w_i a_i(x) V_i} \tag{2}$$

depended on then-part set B_j only through its volume or area V_j (and perhaps through its rule weight w_j). We note that (1) and (3) below imply [3] that $F(x) = E[Y|X = x]$. So the SAM output describes the *first-order* behavior of the fuzzy system and does not depend on the shape of the then-part sets B_j. But the shape of B_j did affect the *second-order* uncertainty or conditional variance $V[Y|X = x]$ of the SAM output $F(x)$ [3]:

$$V[Y|X = x] = \sum_{j=1}^{m} p_j(x) \sigma_{B_j}^2 + \sum_{j=1}^{m} p_j(x)(c_j - F(x))^2 \tag{3}$$

DEPTH	MOMENTUM							
WEIGHT		VS	SM	MS	MD	ML	LG	VL
	VL	MD	MD	MD	LG	LG	LG	VL
	LG	MD	MD	MD	LG	LG	LG	VL
	ML	MD	MD	MD	MD	MD	MD	LG
	MD	SM	MD	MD	MD	MD	MD	LG
	MS	SM	SM	SM	SM	SM	MD	LG
	SM	SM	SM	SM	SM	SM	MD	MD
	VS	VS	VS	VS	SM	SM	MD	MD

TABLE II. **Initial fuzzy rules for the depth subsystem. The initial fuzzy rules for the armor-deformation depth based on the experimenters' ballistic judgment and experience. A typical rule was "If the bullet's weight is very small (VS) and the momentum is small (SM) then the armor deformation depth is SM and the width is VS." The if-part fuzzy sets describe the bullet's weight {Very Small, SMall, Medium Small, MeDium, Medium Large, LarGe, Very Large} and momentum {VS, SM, MS, MD, ML, LG, VL}. The then-part fuzzy sets describe the armor deformation's depth {VS, SM, MD, LG, VL} and width {VS, SM, MD, LG, VL}.**

where $\sigma_{B_j}^2$ is the then-part set variance

$$\sigma_{B_j}^2 = \int_{-\infty}^{\infty} (y - c_j)^2 p_{B_j}(y) dy \tag{4}$$

where $p_{B_j}(y) = b_j(y)/V_j$ is an integrable probability density function, and where $b_j : R \to [0, 1]$ is the integrable set function of then-part set B_j. The first term on the right side of (3) gave an input-weighted sum of the then-part set uncertainties. The second term measured the *interpolation penalty* that resulted from computing the SAM output $F(x)$ in (1) as the weighted sum of centroids. The second-order structure of a fuzzy system's output depends crucially on the size and shape of the then-part sets B_j. Fig. 4 shows the conditional-variance surface of the depth output.

We used scalar Gaussian set functions for the one-dimensional then-part fuzzy sets B_j. This gave the set variance $\sigma_{B_j}^2$ from the then-part set volume $V_j : \sigma_{B_j}^2 = V_j^2/2\pi$.

We used the 2-D factorable sinc function (see Fig. 3) for the if-part fuzzy sets A_j. Sinc sets often converge faster and with greater accuracy than do triangles, Gaussian bell curves, Cauchy bell curves, and other familiar set shapes [21].

A larger then-part rule volume V_j produced more uncertainty in the j^{th} rule and so should result in less weight. So we weighted each rule with the inverse of its squared volume [3]: $w_j = 1/V_j^2$. A larger volume V_j also gave a larger conditional variance.

We picked the fuzzy system's initial rules according to the observed correlations in Table 1: Same-weight bullets hit harder if they were faster. Same-speed bullets hit harder if they were heavier. But heavier and slower handgun bullets hit harder than lighter and faster ones. The if-part set functions a_j used center and width parameters to uniformly cover the input space. The then-part set functions b_j used center parameters or centroids c_j that gave an output according to Table 2 and used width parameters that reflected the uncertainty of the rules. The fuzzy sets in Table 2 listed the initial rules we created based on our experience with ballistics and soft body armor. The volume V_j was a function of its width parameter. A rule was less certain if its if-part covered untested combinations of bullet weight and momentum so its then-part had a larger

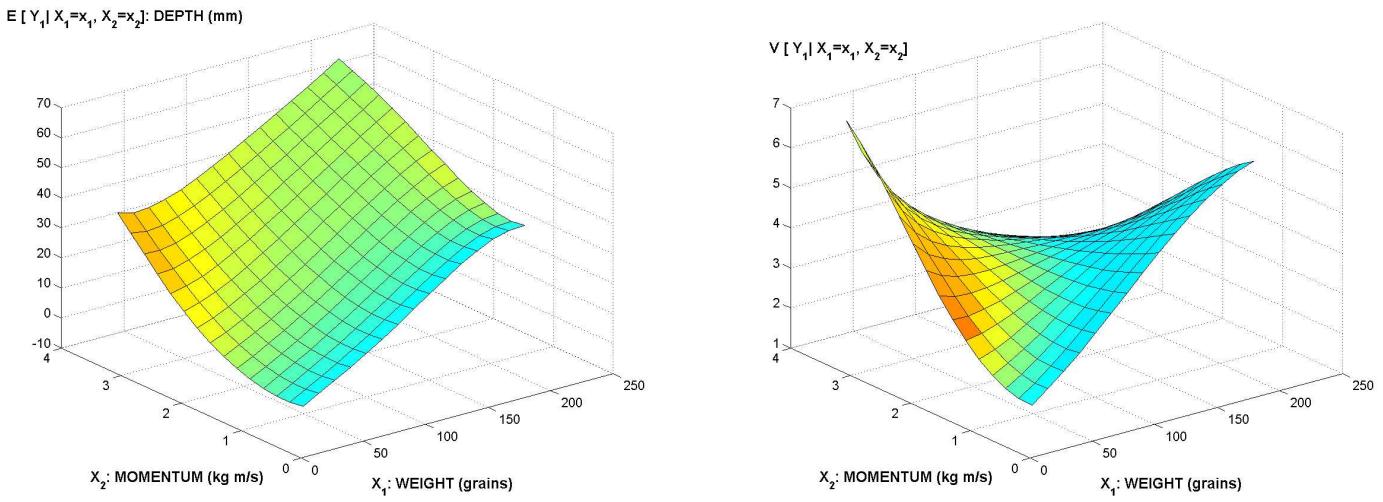

Fig. 4. **Fuzzy system output and conditional variance. An adaptive fuzzy system used two parallel scalar fuzzy systems to model the depth and width (mm) of a bullet-armor deformation given the bullet's weight (grain) and momentum (grain feet per second). The experiments used one weight per bullet caliber so that a bullet's weight could represent its caliber in the input. The output gave the depth and width of the bruise profile. Each surface plots the output against the momentum to the left and the weight to the right. The first-order outputs are the depth and width. The second-order uncertainties are the conditional variance for the depth and width. We initialized the fuzzy rules using correlations in the experimental data (see Table 2). The left and right side rules were less certain because their if-parts covered untested combinations of bullet weight and momentum. So their then-parts had larger set variances and gave larger conditional variances. (a) The depth output surface (b) The conditional variance of the depth output. The width subsystem produced similar surfaces. Both the depth and width increased as the bullet weight and momentum increased.**

set variance. Fig. 4 shows the fuzzy system's initial first-order output $F(x) = E[Y|X = x]$ and second-order uncertainty $V[Y|X = x]$.

A random resampling scheme selected two thirds of the sparse data as the bootstrapped training set and the remaining one third as the test set [22]. A bootstrap scheme sampled the training data with replacement at random to generate 300 sets of input-output data to tune the fuzzy system.

Tuning reduced the system's error function that summed the squared differences (SSE) between the training data and the output by more than a half for 3000 epochs of learning: It reduced the depth subsystem error from 38 to 11.6 and reduced the width subsystem error from 47 to 21. The final SSE resembled the initial SSE. Test data produced the low test error of SSE = 20.5 for the depth subsystem and so showed that the tuning was effective. Learning only slightly improved the width subsystem because the test error of SSE = 42 was only slightly less than the initial error of 47.

The fuzzy system was robust against random pruning (see Fig. 5). Pruning randomly removed a fraction of the rules over 100 trials. The depth and the width subsystems gave similar results. The maximal test error remained low (SSE < 100) for up to 20 percent of randomly removed rules. This was comparable to the approximation errors in data tuning. Both the mean and the median of the test error remained low for random pruning that removed up to 30 percent of the rules.

V. BULLET-ARMOR IMPACT EXPERIMENTS

The bullet-armor experiments found that the a bullet-armor impact's depth and width correlated with the combination of the bullet's weight and momentum. The regression statistics were $R^2 = 0.953$ for the depth and $R^2 = 0.951$ for the width.

A bullet's impact depth and width correlated better with its momentum mv than with its weight m, speed v, or kinetic energy $\frac{1}{2}\, mv^2$ (Table 1). A bullet's weight could represent its caliber in the fuzzy system because the experiments used one weight per bullet caliber. So the fuzzy system's inputs were weight and momentum.

Linear regression measured how well the bullet-armor data fit a straight line. The null hypothesis $\mathbf{H}_0 : \beta_1 = 0$ stated that the slope β_1 of the regression line was zero and thus the impact deformation's depth and width (dependent variables) did not vary with a bullet's weight, speed, momentum, or kinetic energy (independent variables). The p-value measures the credibility of $\mathbf{H}_0$. A statistical test rejects the null hypothesis $\mathbf{H}_0$ at a significance level α if the p-value is less than that significance level: Reject $\mathbf{H}_0$ if p-value $< \alpha$. So the regression rejected the null hypothesis $\mathbf{H}_0$ at the standard significance levels $\alpha = 0.05$ and $\alpha = 0.01$ because p-value < 0.001. The depth regression equation was $y = 0.064 + 0.006x_1 + 7.5 \times 10^{-6} x_2$, where x_1 was bullet weight and x_2 was bullet momentum. The width regression coefficients were $\beta_0 = 3.274$, $\beta_1 = 0.002$, and $\beta_2 = 1.8 \times 10^{-5}$.

We used four bullet calibers (.22, .38, .40, and .45 caliber) and two different speeds (such as on average 808 ft/s and 897 ft/s for the .45) per caliber to produce 46 sets of input-output data. This gave a sparse sampling of the input space.

The bullet-armor experiments used eight layers of ballistic fabric for generic armor, blocks of ten-percent ordnance gelatin for tissue simulant, and full-copper-jacket range ammunition for handgun bullets. We made the generic armor with eight layers of Aramid fabric style 713 from Hexcel Schwebel that consisted of 1000 deniers of Kevlar 29 fibers in plain weave.

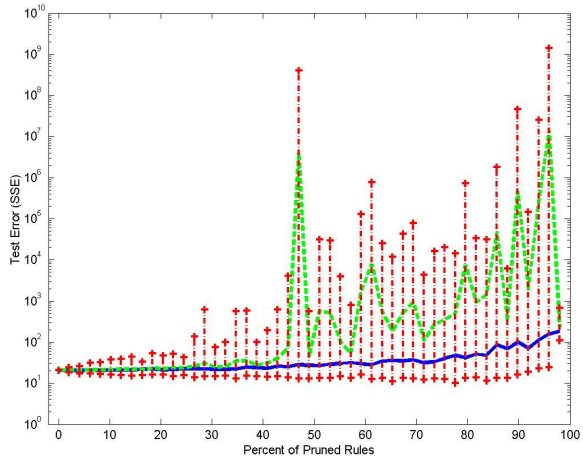

Fig. 5. **Rule pruning. The fuzzy system was robust against random pruning. The figure plots the system's test error in log scale versus the percent of pruned depth rules. Similar result holds for random pruning of width rules. The vertical bars show the maximal and minimal range of 100 trials. The solid polygonal line interpolates the median of those trials. The dashed line interpolates the mean. The maximal error remained below 100 sum squared error (SSE) for up to 20% of randomly pruned rules. Both the mean and median error remained low for rule losses of up to 30%. The tuning was effective for the depth subsystem: Test SSE = 20.5 was less than the initial error of 38. But tuning only slightly improved the width subsystem because the test error of SSE = 42 was only slightly less than the initial error of 47.**

The gelatin blocks consisted of water and Kind & Knox Type 250A Ordnance Gelatin at ten percent by weight. The Orange County Indoor Shooting Range provided the space, the rental handguns, and range ammunition for the experiments.

Handguns with different barrel lengths shot bullets at the armor-clad gelatin blocks over a fixed distance. The experiments recorded at least five shots for each of the seven combinations of bullet weight and mean velocity. An optical chronometer measured the bullet speeds in separate tests and found the mean speed of the bullets from the same ammunition box using the same handguns. The chronometer was the Prochrono Plus model from Competition Electronics.

The gelatin mixture sat for 24 hours to minimize air bubbles. A water bath heated the mixture until the gelatin dissolved while keeping the mixture's temperature below 40 degrees C. A refrigerator cooled the mixture in molds for 48–72 hours to ensure the gelatin blocks had uniform temperature close to 4 degrees C. A BB shot calibrated each gelatin block before use by giving BB penetration at known temperatures.

VI. BASEBALL IMPACT EXPERIMENTS

The baseball impact experiments used regulation baseballs (Fig. 7) to produce at least 10 data points for each of six different speeds. Pitching machines threw the balls at tubs of Oatey's plumber's putty at a distance of 5 feet. Home Run Park in Anaheim provided the batting cages that had baseball speeds from 40 mph to 90 mph. The optical chronometer measured the baseball speeds before the impact in each test. The putty deformed to record each baseball impact.

The baseball experiments found that the mean depth of a baseball's impact correlated with its speed: The statistics

Bullet Caliber	.22	.38	.357	.45
Depth (mm)	5	15	21	22
Baseball Speed (mph)	40	70	80	90
Depth (mm)	6.5	13.6	17	21.6

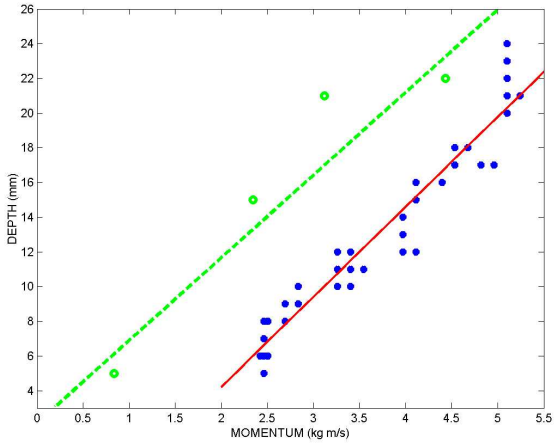

Fig. 6. **Baseball and bullet impact depth in plumber's putty versus momentum. The baseball impact depth correlated with baseball momentum $R^2 = 0.93$ and p-value < 0.001 for the null hypothesis: $\beta_1 = 0$. The solid line on the right is the regression line for the baseball impacts (blue dots) $y = \beta_0 + \beta_1 x$ where x is baseball momentum and y is putty deformation depth for the regression coefficients $\beta_0 = -6.155$ and $\beta_1 = 5.188$. Only two data fell outside of the 95% confidence bounds. Bullet-armor impact depths correlated with bullet momentum $R^2 = 0.97$. The green dashed line on the left is the regression line for the bullet-armor impacts (green circles) $y = 2.124 + 4.766x$ where x is bullet momentum and y is depth. The two regression lines have the similar slope $\beta_1 \approx 5$. Baseballs deformed plumber's putty similar to handgun bullets: The mean impact depth was 21.6 mm for 90-mph baseballs. The bullet-armor impact depth was 21 mm for a .357 magnum bullet and 22 mm for a .45 caliber bullet. The mean depth was 17 mm for 80-mph baseballs and was 13.6 mm for 70-mph baseballs. The bullet-armor depth was 15 mm for a .38 caliber bullet. The mean depth was 6.5 mm for 40-mph baseballs. And the bullet-armor depth was 5 mm for a .22 caliber bullet**.

were $R^2 = 0.93$ for correlation and p-value < 0.001 for the linear regression. The regression equation had the form $y = -6.155 + 5.188x$ where x was baseball momentum and y was putty deformation depth. The correlation was the same between the impact depth and baseball momentum because the baseballs had approximately the same weight. This corroborated the results from the bullet-armor experiments.

Baseball impacts and bullet-armor impacts had similar depths in Oatey's plumber's putty (Fig. 6). The similarity of impact depths suggested that handgun shots on soft body armor would feel like baseball impacts without armor. Fast-baseball impact depths were comparable to bullet-armor impact depths: Getting shot with a .22 caliber bullet when wearing soft body armor resembles getting hit on the chest with a 40-mph baseball. Getting shot with a .45 caliber bullet resembles getting hit with a 90-mph baseball.

VII. CONCLUSION

The adaptive SAM system modeled the bruise profile of a bullet impact based on bullet-armor experiments. The fuzzy system's output conditional variance measured the inherent uncertainty in the rules. A baseball analogy gave further insight into armor gunshots based on baseball-impact experiments.

Fig. 7. **A regulation baseball and a record of its impact. Pitching machines threw baseballs at tubs of plumber's putty. A chronograph measured the speed of each baseball. The baseball speeds were approximately 40, 50, 60, 70, 80, and 90 miles per hour.**

The bullet-armor experiments found correlations between a bullet impact's depth and width and its weight and momentum. The baseball correlations corroborated the bullet-armor results. These results would benefit from further testing with more than one weight per caliber.

APPENDIX

This appendix derives the learning laws for scalar and joint factorable if-part sets. Supervised gradient descent can tune all the parameters in the SAM (1). A gradient descent learning law for a SAM parameter x has the form

$$\xi(t+1) = \xi(t) - \mu_t \frac{\partial E}{\partial \xi} \tag{5}$$

where μ_t is a learning rate at iteration t. We seek to minimize the squared error $E(x) = {}^1\!/_2(f(x) - F(x))^2$ of the function approximation. The vector function $f : R^n \rightarrow R^p$ has components $f(x) = (f_1(x), \ldots, f_p(x))^T$ and so does the vector function $F(x)$. We consider the case when p = 1. A general form for multiple output when $p > 1$ expands the error function $E(x) = \| f(x) - F(x) \|$ for some norm $\|.\|$. Let ξ_j^k denote the k^{th} parameter in the set function a_j. Then the chain rule gives the gradient of the error function with respect to the if-part set parameter ξ_j^k, with respect to the then-part set centroid $c_j = (c_j^1, \ldots, c_j^p)^T$, and with respect to the then-part set volume V_j

$$\frac{\partial E}{\partial \xi_k^j} = \frac{\partial E}{\partial F}\frac{\partial F}{\partial a_j}\frac{\partial a_j}{\partial \xi_k^j}, \frac{\partial E}{\partial c_j} = \frac{\partial E}{\partial F}\frac{\partial F}{\partial c_j}, \text{ and } \frac{\partial E}{\partial V_j} = \frac{\partial E}{\partial F}\frac{\partial F}{\partial V_j} \tag{6}$$

where

$$\frac{\partial E}{\partial F} = -\left[f(x) - F(x)\right] = -\varepsilon(x) and \frac{\partial F}{\partial a_j} = (c_j - F(x))\,\frac{p_j(x)}{a_j(x)}. \tag{7}$$

The SAM ratios (1) with inverse-squared-volume rule weights $w_j = 1/V_j^2$ give

$$\frac{\partial F}{\partial c_j} = \frac{a_j(x)/V_j}{\sum_{j=1}^{m} a_j(x)/V_j} = p_j(x) \tag{8}$$

$$\frac{\partial F}{\partial V_j} = -\frac{p_j(x)}{V_j}\,(c_j - F(x)) \tag{9}$$

Then the learning laws for the then-part set centroids c_j and volumes V_j have the final form

$$c_j(t+1) = c_j(t) + \mu_t \varepsilon_t(x) p_j(x) \tag{10}$$

$$V_j(t+1) = V_j(t) - \mu_t \varepsilon_t(x)\frac{p_j(x)}{V_j}[c_j - F(x)] \tag{11}$$

The learning laws for the if-part set parameters follow in like manner for both scalar and joint sets as we show below. Chain rule gives for scalar sinc set function

$$\frac{\partial E}{\partial m_j^k} = \frac{\partial E}{\partial F}\frac{\partial F}{\partial a_j}\frac{\partial a_j}{\partial m_j^k} \text{ and } \frac{\partial E}{\partial d_j^k} = \frac{\partial E}{\partial F}\frac{\partial F}{\partial a_j}\frac{\partial a_j}{\partial d_j^k} \tag{12}$$

A joint factorable set function $a_j(x) = a_j^1(x) \ldots a_j^n(x)$ leads to a new form for the error gradient. The gradient with respect to the parameter of the j^{th} set function a_j has the form

$$\frac{\partial E}{\partial m_j^k} = \frac{\partial E}{\partial F}\frac{\partial F}{\partial a_j}\frac{\partial a_j}{\partial a_j^k}\frac{\partial a_j^k}{\partial m_j^k} \text{ where } \frac{\partial a_j}{\partial a_j^k} = \prod_{i \neq k}^{n} a_j^i(x_i) = \frac{a_j(x)}{a_j^k(x_k)}. \tag{13}$$

Combining (5), (6), (12), and (13) gives the if-part learning laws.

REFERENCES

[1] *Second Chance Saves*, pp. 7 and 16. Second Chance Inc., Central Lakes, Michigan, 1999.

[2] A. Jason, M. L. Fackler, "Body Armor Standards: A Review and Analysis," *IWBA Wound Ballistics Review*, vol. 1, no. 1, pp. 14–37, 1992.

[3] Kosko, B., *Fuzzy Engineering* Prentice Hall 1996.

[4] D. W. Walsh, J. Hagen, "Body Armor: What it is and what it does," JEMS, pp. 66–67, Sept. 1994.

[5] D. MacPherson, "Dynamic Projectile Interactions and Associated Body Armor Effects," *IWBA Wound Ballistics Review*, vol. 1, no. 4, pp. 29–31, 1994.

[6] M. C. Andrews, R. J. Young, "Fragmentation Of Aramid Fibers In Single- Fiber Model Composites," *Journal Of Materials Science*, Vol. 30, Issue 22, Pp. 5607–5616, Nov 15, 1995.

[7] D. MacPherson, Lt. Ed Fincel Miloskovich, J. Nicholas "Body Armor Penetration Dynamics," *IWBA Wound Ballistics Review*, vol. 3, no. 2 pp. 16– 24, 1997.

[8] P. M. Cunniff, "A semiempirical model for the ballistic impact performance of textile-based personnel armor," *Textile Research Journal*, Vol. 66, Issue 1, Pp. 45–59, Jan 1996.

[9] I. S. Chocronbenloulo, J. Rodriguez, A. Sanchezgalvez, "A Simple Analytical Model To Simulate Textile Fabric Ballistic Impact Behavior," *Textile Research Journal*, Vol. 67, Issue 7, Pp. 520–528, Jul 1997.

[10] R. L. Ellis, F. Lalande, H. Y. Jia, C. A. Rogers, "ballistic impact resistance of sma and spectra hybrid graphite composites," *Journal Of Reinforced Plastics And Composites*, vol. 17, no. 2, pp. 147–164, 1998.

[11] T. E. Bachner, Jr. "The V-50 Ballistic Limit: A Reliable Test for Body Armor," *IWBA Wound Ballistics Review*, vol. 1, no. 4, pp. 20–25, 1996.

[12] D. MacPherson, *Bullet Penetration: Modeling the Dynamics and the Incapacitation Resulting from Wound Trauma*: Ballistic Publications 1994.

[13] D. MacPherson, "The Dynamics of Tissue Simulation," *IWBA Wound Ballistics Review*, vol. 3, no. 1, pp. 21–23, 1997.

[14] M. L. Fackler, J. A. Malinowski, "The Wound Profile: A Visual Method for Quantifying Gunshot Wound Components," *Journal of Trauma*, vol. 25, no. 6, pp. 522–9, 1985.

[15] A. J. Ryan MD, "Traumatic injuries: Office treatment of deep bruises," *Postgraduate Medicine*, Vol. 59, no. 6, Pp. 195–197, 1976.

[16] G. A. Galanti, *Caring for patients from different cultures (2nd ed.)*, Philadelphia: University of Pennsylvania Press 1997.

[17] T. Stephenson, Y. Bialas, "Estimation of the age of bruising," *Archives of Disease in Childhood*, vol. 74, no. 1, pp. 53–5, Jan 1996.

[18] V. B. Pai, M. W. Kelly, "Bruising associated with the use of fluoxetine," *Annals of Pharmacotherapy*, Vol. 30, No. 7–8, pp. 786–788, 1996.

[19] A. W. Carroll, C. A. Soderstrom, "A new nonpenetrating ballistic injury," *Annals of Surgery*, vol. 188, no. 6, pp. 753–757, Dec 1978.

[20] G. C. Velmahos, R. Tatevossian, D. Demetriades, "The seat belt mark sign: A call for increased vigilance among physicians treating victims of motor vehicle accidents," *American Surgeon*, Vol. 65, no. 2, pp. 181–5, 1999.

[21] S. Mitaim, B. Kosko, "The shape of fuzzy sets in adaptive function approximation," *IEEE Transactions on Fuzzy Systems*, vol. 9, no. 4, pp. 637– 656, August 2001.

[22] A. M. Zoubir, B. Boashash, "The bootstrap and its application in signal processing," *IEEE Signal Processing Magazine*, pp. 56–76, Jan 1998.